

Contents lists available at ScienceDirect

Chemosphere

journal homepage: www.elsevier.com/locate/chemosphere





Application of dimensional analysis in sorption modeling of the styryl pyridinium cationic dyes on reusable iron based humic acid coated magnetic nanoparticles

Anahita Esmaeilian, Kevin E. O'Shea*

Department of Chemistry and Biochemistry, Florida International University, 11200, SW 8th Street, Miami, FL, 33199, USA

HIGHLIGHTS

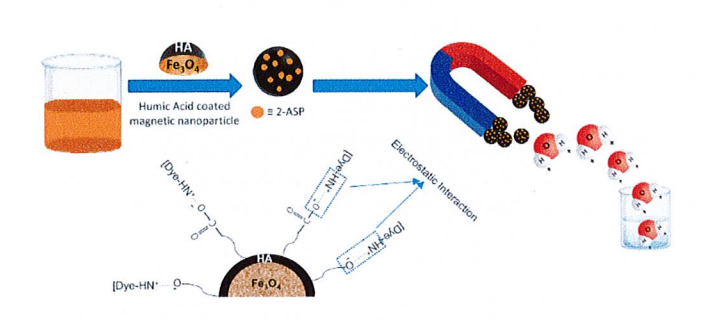
- Humic acid coated magnetic nanoparticles effectively remove styryl pyridinium dyes.
- Adsorption fits with the pseudo secondorder kinetic and Langmuir isotherm models.
- The initial concentration/sorbent dose ratio is proposed as a controlling variable.
- NaOH treatment of HA-MNP modify the surface to enhance the adsorption capacity.

ARTICLEINFO

Handling Editor: Chang Min Park

Keywords: HA-MNPs 2-ASP dye Remediation Regeneration Dimensional analysis

GRAPHICAL ABSTRACT



ABSTRACT

Cationic dyes exist in various industrial wastewaters and removal prior to discharge is necessary due to their carcinogenic behavior which poses a serious threat to human health. Iron based humic acid coated magnetic nanoparticles (HA-MNPs) were evaluated for the removal of 2-[4-(dimethylamino) styryl]-1-methylpyridinium iodide (2-ASP) as a model compound for cationic styryl pyridinium dyes from aqueous media. HA-MNPs were prepared by co-precipitation and characterized. The adsorption of 2-ASP, measured by fluorescence, demonstrates HA-MNPs are efficient for the 2-ASP removal with a maximum adsorption capacity of ~8 mg/g. Kinetic behavior and equilibrium studies showed the adsorption process fits with pseudo 2nd order and Langmuir isotherm models. The adsorption is relatively fast with $\sim 70\%$ of the adsorption complete within 30 min. The overall removal increases by increasing solution pH. The observed increase in adsorption can be assigned to an enhanced electrostatic attraction between the positively charged 2-ASP and the increase in the negative charge on the HA-MNPs surface as a function of increasing solution pH. Effective and repetitive regeneration of the HA-MNPs was achieved using NaOH treatment of saturated sorbent. Regeneration of HA-MNPs showed that removal efficiency remains consistently high after five consecutive cycles. Dimensional analysis suggested that initial concentration/sorbent dose ratio should be considered for accurate sorption modeling confirmed by experimental data. Then generalized empirical models for isothermal study and removal efficiency prediction were accurately deduced. This finding will help researchers in sorption studies to design their experiments more efficiently and to develop improved empirical models in removal prediction.

^{*} Corresponding author. E-mail addresses: aesma009@fiu.edu (A. Esmaeilian), osheak@fiu.edu (K.E. O'Shea).

1. Introduction

Cationic dyes, extensively used in textile, rubber, paper industries, leather, gasoline, pharmaceutical, and food industries, are sources of serious concern in aquatic environments and biological systems (Brahim et al., 2021; Ding et al., 2021; Kausar et al., 2021; Sakti et al., 2020). These dyes can pass through negatively charged cell membranes and accumulate in the cytoplasm (Bayramoglu et al., 2009; Oseroff et al., 1986) leading to damage of the nervous systems of living organisms. Cationic dyes are toxic even at trace levels due to the formation of metal-chelate complexes (Al-Degs and Sweileh, 2012; Peng et al., 2012). Once these toxic dyes enter the food chain, bioaccumulation processes threaten higher organisms including humans. In addition, a number of dyes produce byproducts upon degradation which are highly carcinogenic (Puvaneswari et al., 2006; Zhou et al., 2019). Unfortunately, a number of these dyes are also highly resistant to transformation and thus can persist in water for extended periods (Deng et al., 2021). The United States Environmental Protection Agency (EPA) set a Maximum Contaminant Level (MCL) of 1.0 μ g L⁻¹ in drinking water for cationic dyes (Al-Degs and Sweileh, 2012). Cationic dyes are a threat to the environment and human health thus their removal from industrial wastewater is critical before release into natural aquatic systems.

Among the remediation methods such as oxidation (Zhu et al., 2018), sedimentation (Huang et al., 2019), photodegradation (Qian et al., 2021), adsorption is one of the most commonly used methods especially when economical sorbents with high surface area are identified. A number of adsorbents have been used for removal of dyes from aqueous media, including nanocomposite based on octa-amino polyhedral oligomeric silsesquioxanes, carbon nanotubes, and chitosan (Zhao et al., 2021), activated carbon (Allen and B. Koumanova, 2005), and silica gel (Parida et al., 2006). Advances in nanotechnology and the development of magnetic nanoparticles (MNPs) show great potential to produce an adsorbent with large surface area and small diffusion resistance characteristics. MNPs have been used as bare or coated particles for removal of dyestuffs from wastewater (Ge et al., 2012). Glutamic acid modified chitosan- and silica-coated Fe₃O₄ nanoparticles (Yan et al., 2013), magnetic peach gum bead bio-sorbent (Li et al., 2018), superparamagnetic nanoparticles coated with green tea polyphenol (Singh et al., 2017), synthesized hybrid of microporous organic polymer and sodium acrylate hypercrosslinked polymer with magnetic Fe₃O₄ nanoparticles (Li et al., 2017) have been used to remove cationic dyes including Rhodamine B, methylene blue and crystal violet from wastewater. MNPs are subject to deterioration due to oxidation and aging processes, thus coating MNPs can inhibit auto-oxidation, reduce agglomeration and extend the functional lifetime of the particles. Humic acid, a fraction of natural organic matter (NOM), is an attractive coating which can be applied in an environmentally friendly process. Humic acid has the strong sorption capacity for anions and cations (Liu et al., 2008; Rashid et al, 2017, 2018). There are only a limited number of reports on the adsorption of dyes by HA-MNPs from aqueous media (Gautam and Tiwari, 2020; Peng et al., 2012). Results of Peng et al. revealed that HA-MNPs have a high potential as an efficient nanomaterial for removal of RhB from water (Peng et al., 2012). Gautam et al. showed the rapid removal of malachite green by HA-MNPs under ultrasonic irradiation with ~100 % removal over a range of concentrations.

In the current study, HA-MNPs were synthesized, characterized and studied for the removal of 2-[4-(dimethylamino) styryl]- 1- methylpyridinium iodide (2-ASP) as a model of styryl pyridinium cationic dye from aqueous media. 2-ASP has higher $\mathrm{LD_{50}}=491$ mg/kg (mouse, oral) and moderate toxicity compared to other common styryl cationic dyes such as SP-1 (typical cyanine dye) (Guru and Dash, 2012). The model dye, 2-ASP, has strong fluorescent properties making readily detectable even at very low concentrations. Removal of styryl pyridinium dyes to these low levels would ameliorate the risks of bioaccumulation. To examine the adsorption process and capacity of this magnetic sorbent, individual

equilibrium and kinetic batch studies were performed. The objective of this work was to investigate the removal of 2-ASP with HA-MNPs, and a develop an effective process to regenerate and reuse the HA-MNPs.

2. Materials and methods

2.1. Materials

The chemicals, ammonium hydroxide (29.15 %), ferric chloride hexahydrate (FeCl₃·6H₂O) (98.8 %), methanol (OptimaTM), glacial acetic acid, sodium hydroxide (NaOH) were reagent grade and purchased from Fisher scientificTM. Humic acid sodium salt and ferrous chloride tetrahydrate (FeCl₂·4H₂O) \geq 99.0 % were obtained from Sigma-Aldrich. Millipore water (MilliQ water, resistivity~18.0 M Ω cm⁻¹ at 25 °C) was used for all experiments. 2-[4-(dimethylamino) styryl]-1-methylpyridinium iodide (2-ASP) (MW; 366.24 g/mol, λ max: 583 nm) was supplied by Fisher ScientificTM and its chemical structure illustrated in Fig. S1.

2.2. Synthesis of humic acid-coated magnetic nano particle

Humic acid coated magnetic nanoparticles were synthesized following an established co-precipitation method (Liu et al., 2008). Briefly, 6.0 g of ferric chloride hexahydrate (FeCl₃·6H₂O) and 3.1 g of ferrous chloride tetrahydrate (FeCl₂·4H₂O) were added to 100 mL of deionized water in a three-neck flask equipped with a reflux condenser and heated to 90 °C then 10 mL of 25 % ammonium hydroxide and 50 mL of 1 % humic acid sodium salt were added in quick succession into the reaction mixture, respectively. Temperature was kept at 90 \pm 5 $^{\circ}$ C for an additional 30 min. The mixture was allowed to cool to room temperature and washed several times with Millipore filtered water to obtain the natural pH and remove free, unreacted humic acid from the particles. The precipitated HA-MNPs were then dried in a vacuum oven at room temperature for at least a week. The dried materials were ground with a pestle to a fine powder. The uncoated magnetic nanoparticles (Fe₃O₄) were synthesized following the same procedure without adding the humic acid.

2.3. Characterization of the synthesized nanoparticles

The morphology of the synthesized nanomaterials was characterized by the Transmission Electron Microscopy, TEM, (Philips CM200 operated at 200 keV), the Scanning Electron Microscopy, SEM, (EOL 6330F, operated at 25.0 keV). BET (N2) method was used for surface area measurement (Micromeritics TriStar II (TriStar II 3020 V1.03) gas adsorption analyzer). The attenuated total reflectance Fourier Transform Infrared Spectroscopy (ATR-FTIR) was performed at room temperature using PerkinElmer FTIR 100. Spectral scans of the synthesized nanoparticles were obtained from 400 to 4000 cm^{-1} (64 scans per spectrum). The leaching of iron from HA-MNPs was determined by measuring free iron in solutions after the sorption process and separation of the synthesized HA-MNPs using PerkinElmer NexION 2000 ICP-MS. The leaching of HA into the water was determined by measuring Total Organic Carbon (TOC) in solution after separation of HA-MNPs. TOC was measured by the Non-Purgeable Organic Carbon (NPOC) method and measurements taken on a Shimadzu TOC-VCSH analyzer. The zeta potentials of uncoated, coated magnetic nanoparticles pre and post treatment were determined using a Malvern Zetasizer Nano Z. The zeta potentials were recorded for MNPs and HA-MNPs at solution pH from ~2 to 10.

2.4. Adsorption experiment

A stock solution of 2-[4-(dimethylamino) styryl]-1-methylpyridinium iodide (2-ASP) at a concentration of 1000 mg/L was prepared by dissolving the appropriate amount of dye in the 1000

mL of Millipore filtered water. Kinetic studies were performed in batch mode using 15-mL capped flasks to determine the sorption of 2-ASP. A solution of 2-ASP at desired concentration was prepared and 10 mL transferred into the flasks containing fixed concentration of HA-MNP (0.01 g/10 mL). The samples were shaken at 300 rpm with orbit shaker (Lab-line instrument Inc., model 3520) for 5, 15, 30, 60, 90, 120, and 180 min to ensure that the adsorption equilibrium is completed. 2-ASP concentrations were measured after separation of nanoparticles by a handheld magnet and/or filtration by using 0.45 μm syringe filter. The 2-ASP concentrations were measured at $\lambda_{em} = 583$ nm by using Cary Eclipse Fluorescence Spectrophotometer (Agilent Technologies). Proper dilutions were performed before measurement to ensure that dye concentrations were within the linear range of the standard calibration curve (500 ppb-3 ppm). To estimate the kinetic sorption parameters, non-linear least-square method was used. In non-linear method, the kinetic parameters were estimated by minimizing the sum of square errors between experimental data and kinetic model using the solver add-in Microsoft Office 365 Excel spreadsheet.

Equilibrium experiments were carried-out as a function of initial concentrations of 2-ASP, sorbent dose, and solution pH. Adsorption equilibrium tests were carried out using capped flasks shaken for 2 h. Initial experiments established that 2 h assured adsorption equilibrium between 2-ASP and HA-MNPs under our experimental conditions occurred. The initial solutions were prepared by dilution of the 2-ASP stock solution over the range of 3–30 mg/L. All experiments were conducted at room temperature (298 K) at solution pH 7.1 \pm 0.1. To investigate the influence of solution pH on the adsorption 0.1 M NaOH and HCl solutions were used to adjust the initial solution pH monitored by a pH meter (Mettler Toledo, model SevenEasy). For the thermodynamic study, sample solutions were placed in the Brunswick Innova 3100 Waterbath shaker to maintain the desired temperature.

The amounts of ions adsorbed by HA-MNPs, q (mg/g), were determined from the measured dye concentrations remaining in the solution, using the following equation:

$$q_t \text{ or } q_e = \frac{(C_0 - C_{e \text{ or } t}) \forall}{W} \tag{1}$$

where \forall (I) is the solution volume, W (g) is the weight of HA-MNPs, C_0 (ppm) is the initial dye concentration and $C_{e\ o\ t}$ (ppm) is the equilibrium concentration of the solution or bulk concentration at indicated time respectively. All experiments were carried out in triplicate and exhibit at least 95 % confidence interval. Sum of square error (SSE) are used, to evaluate models (Equation (2)).

$$SSE = \sum_{i=1}^{N} (O_i - P_i)^2$$
 (2)

where P_i and O_i are the calculated and measured amounts of adsorbed substrate respectively.

2.5. Desorption and regeneration

Regeneration and reuse of the humic acid coated magnetic nanoparticle is important from economic and environmental sustainability perspectives. Regeneration experiments were conducted using a mixture of methanol and acetic acid with volume ratio of 9:1 (Zhang et al., 2013). The dye-saturated HA-MNPs (1 g/L) were added to the regeneration medium and were shaken for 20 min. Although desorption of dye from sorbents was very fast, this process was repeated with a fresh batch of regenerating agent to ensure complete removal of residual 2-ASP from the HA-MNPs surface prior to the next adsorption-desorption cycle. The recovered adsorbent was then washed by deionized water, and reactivated by 0.1 mol/L NaOH aqueous solution. The NaOH solution was slowly titrated into the regenerated HA-MNPs until a solution pH 9.5 \pm 0.5 was obtained. The alkaline treated HA-MNPs were rinsed with deionized water to obtain neutral pH. The resulting HA-MNPs were

vacuum dried at room temperature and subsequently cycled through the adsorption-desorption process.

3. Result and discussion

3.1. Characterization of the synthesized nanoparticles

The HA-MNPs were characterized initially, after use and after regeneration. The ATR-FTIR spectra of humic acid and humic acid coated and uncoated magnetic nanoparticles are shown in Fig. S2. The zeta potentials of uncoated and coated magnetic nanoparticles were measured by Electrophoretic Light Scattering (ELS) as a function of solution pH. The pH of zero point charge (pH_{PZC}) of Fe₃O₄ was 5.8 (Fig. S3) which is close to that reported in literature with $pH_{PZC} = 6.0$ (Liu et al., 2008). The pH_{PZC} of HA-Fe₃O₄ was 3.7 due the presence of abundant carboxylic acid functional groups in the HA coating. The zeta potential of HA-Fe₃O₄, indicates significant negative surface charge above pH 3.7 which inhibits the aggregation (Gautam and Tiwari, 2020; Liu et al., 2008). Therefore, under neutral and alkaline conditions, HA-Fe₃O₄ is an attractive sorbent for remediation of positively charged ions. BET measurements revealed the surface areas for Fe₃O₄ and HA-Fe₃O₄ are 101.97 and 90.71 (m²/g) respectively, slightly higher than the literature report (Gautam and Tiwari, 2020). These differences are attributed to slight differences in the protocol and ratio of initial materials used in the synthesis (FeCl₃·6H₂O/FeCl₂·4H₂O). The modest decrease in surface area is likely a result of narrow microporosity of HA which leads to no adsorption of N2 at 77 K.

TEM images of the synthesized nanoparticles are shown in Fig. S4 with the core of the magnetic nanoparticle having an average width of \sim 8 nm. The HA-Fe₃O₄ particles had spherical type geometry with sizes (10–24 nm) consistent with literature reports (Gautam and Tiwari, 2020; Liu et al., 2008). Careful examination of Fig. S4 reveals the presence of a thin film (1–4 nm) of humic acid around the iron core (on average \sim 1.67 nm). In addition, the SEM image of bare and coated Fe₃O₄ is shown in Fig. S5. The average size particle for HA-Fe₃O₄ is \sim 16.6 nm which agrees with TEM result. In powdered form significant agglomeration is observed in uncoated magnetic nanoparticle with average individual particle size of 20 nm (Liu et al., 2008).

3.2. Stability of nanoparticles at different dye concentrations and effect of direct photolysis on 2-ASP

Although the amount of iron in drinking water affects its palatability, iron toxicity is exceedingly less common than is iron deficiency in humans. Iron deficiency increases the absorption, potentially leading to toxicity, of other divalent metals, including lead, cadmium, and manganese (Nunamaker et al., 2013). The amount of dissolved iron concentrations leached from sorbent at different concentrations of dye in natural pH were measured by ICP-MS. HA-MNPs (1 g/L) were dispersed with different dye concentrations (3, 10, 15, 20, and 25 mg/L of 2-ASP) and shaken for 2 h. Filtered samples were analyzed to measure the free iron. Table S1 shows the percentage of the iron leaching after suspension of the HA-MNPs at different dye concentrations, showing the amount of iron leaching is negligible. The results indicate the thin relatively uniform HA film observed on the HA-MNP may inhibit leaching of iron from the magnetic core. Moreover, the HA film on the surface of iron oxide nanoparticle at pH above pHPZC may enhance HA binding to Fe3O4 thus reducing leaching iron compared with uncoated magnetic nanoparticles (Vermeer et al., 1998).

The leaching of humic acid from nanoparticle into water during adsorption process was also measured by preparing a mixture of 100 ppm water dispersed HA-MNPs at different solution pH (3, 7 and 10). To simulate the original experimental conditions, the samples were shaken in an orbit shaker at 300 rpm for 2 h. The supernatant was filtered with 0.45 μ m membrane filter and finally analyzed in the TOC analyzer. The concentration of dissolved organic carbon (DOC) along with the amount

of HA correlated with TOC is shown in Table S2. Results show the HA-MNPs is a stable sorbent under different environmental conditions.

2-ASP is a very stable dye under visible or/and UV illumination when dissolved in a solution containing only dye and no nanoparticles. The absorption features showed no significant signs of spectral intensity loss, throughout a 2-h irradiation period (Fig. S6). The results indicate that light has no effect on degradation and the removal mechanism must primarily be adsorption to the HA-MNPs.

3.3. Adsorption kinetics

Kinetic studies were performed to determine the sorption rate of 2-ASP over a range of initial concentrations (5, 15, and 30 ppm) at a fixed concentration of HA-MNPs (1 g/L). The temporal concentration changes in solution for different initial concentrations of 2-ASP are shown in Fig. S7. The adsorption of 2-ASP to HA-MNPs increased with time. Adsorption of 2-ASP is relatively fast with ~70 % of the adsorption complete within 60 min at an initial concentration of 5 ppm (Fig. S7). At higher initial dye concentrations, the adsorption rate was slower and surface saturation was observed (Fig. S7).

The adsorption of 2-ASP versus time was plotted as shown in Fig. 1A. The kinetic studies of 2-ASP sorption exhibit a two-stage time dependent behavior with an initial period of rapid adsorption followed by a slower phase with ≥ 90 % of the removal within the first 30 min. The two-stage process is explained by an initial adsorption on the surface, until all surface sites are occupied, followed by diffusion, migration and/or reorganization at the surface and/or within the HA film as slow adsorption processes. Similar sorption behaviors were reported for sorption of methylene blue (MB) to Fe₃O₄ nanoparticles coated with green tea polyphenols (Singh et al., 2017), MB, crystal violet (CV) and cationic light yellow 7 GL (7 GL) to magnetic composite microsphere (Yan et al., 2013), CV, MB and malachite green (MG) to humic acid (Zhang et al., 2020).

Fig. 1a illustrates equilibrium times vary with initial 2-ASP concentrations. The equilibrium time is determined by t-test analyses of the two last consecutive points for each concentration in Fig. 1a. The result of t-test showed that the differences between adsorbed concentrations at the two last consecutive points are not statistically significant (P > 0.05). The equilibrium adsorption time is 120 min for 30 ppm dye while at 5 and 15 ppm concentrations, equilibrium was achieved within approximately 60 min. The faster observed equilibrium time at lower concentrations can be attributed to the mass transfer limitations. An increase in equilibrium time with initial concentration has been reported for a number of adsorbents (Bahrudin et al., 2019; Li et al., 2018). Based on these results an equilibrium time of 120 min was employed for the experiments in our study. Removal of Direct Blue 2B and Green B dyes from dyeing wastewater collected from a textile dyeing factory in

Calcutta showed that the contact time for equilibrium was also ~120 min (Malik, 2004). A number of sorbents such as activated carbon/cellulose biocomposite films and chitosan/nano-lignin based composite have been used in industry to remove dyes but require long equilibrium times up to 24 h (Sohni et al., 2019; Somsesta et al., 2020).

We applied pseudo-first-order and pseudo-second-order kinetic models to the experimental data to determine the kinetic sorption parameters using Eqs (3) and (4) (Ho and McKay, 1998, 1999).

$$q_t = q_e \left(1 - e^{-k_1 t} \right) \tag{3}$$

$$q_{t} = \frac{k_{2}q_{c}^{2}t}{1 + k_{2}q_{c}t} \tag{4}$$

where k_1 and k_2 is the pseudo-first-order and pseudo-second-order rate constant, q_t and q_e are the amounts of adsorbed 2-ASP at time t and the equilibrium time, respectively.

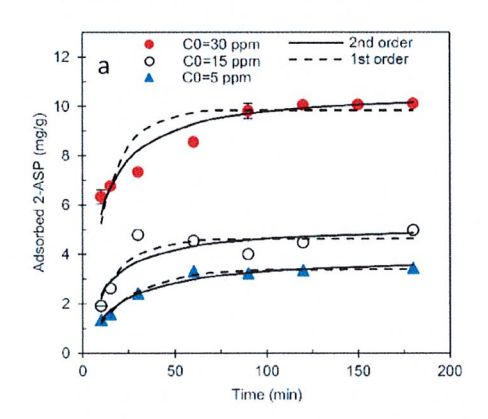
While application of least-squares method to the linear transformed can be used to estimate kinetic sorption parameters for pseudo 1st or 2nd order models, Ho (2006) showed it is better to use a non-linear least-squares method for the original non-linear equation (Ho, 2006; Mahdavi et al., 2013; Nasrabadi et al., 2017; Shahriari et al., 2018). The SSE for kinetic models and the rate constants derived from kinetic equations based on non-linear method are summarized in Table S3. Our results of the pseudo 1st and 2nd order models are summarized in Fig. 1a. Based on SSE in Table S3, the pseudo-first order and pseudo second order models are a good representation adsorption system consistent with previous reports for different sorbates (Chen et al., 2015; Gautam and Tiwari, 2020; Li et al., 2019).

The change in the adsorbed concentration onto adsorbent with time can be probed employing the Weber and Morris intraparticle diffusion model represented by equation (5) below:

$$q_t = K_{id}t^{1/2} + c \tag{5}$$

where K_{id} is the rate constant of intraparticle transport (mg g⁻¹ min^{-1/2}) and c is intercept.

The intraparticle diffusion model plot of q_t versus $t^{1/2}$ is shown in Fig. 1b and intraparticle diffusion rate constant K_{id} was calculated from the slope provided in Table S4. The value of the intercepts indicate the thickness of the boundary layer (Boparai et al., 2011), which has the greater effect on boundary layer and rate limiting step of the process (Kavitha and Namasivayam, 2007). The intraparticle diffusion model demonstrates a two-step sorption process and revealed that intraparticle diffusion is part of the adsorption process although not rate limiting. The initial step is the rapid adsorption at the active sites on the surface. The second level of the adsorption is intraparticle diffusion where dye molecules diffuse slowly into the pores and voids of HA-MNPs as the process approaches equilibrium. The results of Konicki et al. showed



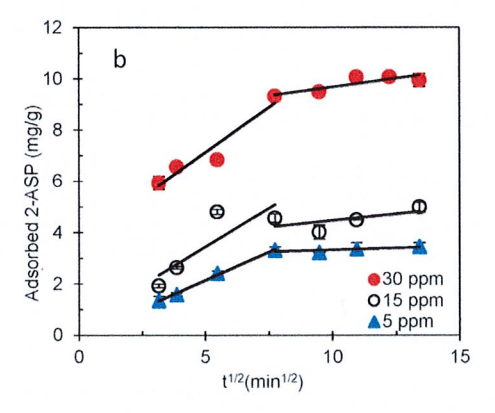


Fig. 1. (a) Adsorption kinetics of 2-ASP on HA-MNPs. (b) 2-ASP adsorption modeling of the kinetic data with Weber-Morris intraparticle diffusion plot. (Initial dye concentration = 5-30 mg/L (ppm), pH = 7.1, HA-MNP dose = 1.0 g/L, temperature = 298 K, contact time = 3 h).

that intraparticle diffusion of the anionic dyes to magnetic Fe@graphite nanocomposite also occurred in two steps of adsorption (Konicki et al., 2017).

3.4. Adsorption isotherms

Equilibrium batch experiments were performed to investigate the effect of initial 2-ASP concentration, solution pH, and sorbent loading. The initial dve concentration has pronounced effect on adsorptive removal processes. The effect of initial dye concentration was investigated in the removal of the 2-ASP dye at 1 and 2 g/L of sorbent. The initial 2-ASP concentrations were 3, 5, 10, 15, 20 and 25 ppm for sorbent loading of 1 g/L and 10, 15, 25, 35, 45 and 55 ppm for sorbent dose of 2 g/L. The percent removal decreases with increasing initial dye concentration, as illustrated in Fig. S8. The results show that the increase of the sorbent dose is most effective at higher concentration of dye. For example, removal percent at 25 ppm increases ~99 % (from ~25 % to ~ 49 %) by increasing sorbent dose (from 1 to 2 g/L), while removal percent increases only ~ 50 % (from ~ 51 % to ~ 77 %) for the same increase in sorbent dose at 10 ppm. Therefore, in applying to wastewater treatment, it is more economical to use a proportionally lower sorbent dose at lower dye concentration. Based on our results, suggest sorbent dose of 1 g/L at dye concentrations lower than 15 ppm may be more economical.

The adsorption isotherm was fitted to Langmuir and Freundlich models (Equations (6) and (7)) (Azizian, 2004) to determine the equilibrium adsorption and the maximum adsorption capacity.

$$q_{c} = \frac{K_{qm}C_{e}}{1 + KC_{e}} \tag{6}$$

$$q_e = kC_e^n \tag{7}$$

where C_e is the supernatant concentration at the equilibrium state of the system (mg/L), K is the Langmuir affinity constant which is related to the adsorption free energy (L/mg), q_m is the maximum adsorption capacity of the sorbent (mg/g), k is the Freundlich constant related with adsorption capacity, and n is the Freundlich exponent. Parameters were calculated based on nonlinear least square method.

Fig. 2 shows the loading of absorbent material versus equilibrium concentration for 1 and 2 g/L of sorbent. With increasing concentration, the amount of adsorbed dye per unit weight of sorbent increases. The Langmuir isotherm model assumes uniform and monolayer adsorption on the surface (no multilayer or clustering of adsorbed molecules). In addition, adsorption occurs in homogeneous adsorbent surface molecules which all sites on the surface are equivalent (Langmuir, 1918). The Freundlich isotherm model however, can accommodate heterogeneity

with multilayer adsorption and non-uniform active sites on the surface of the sorbent. (Freundlich, 1906).

The adsorption parameters and sum of square errors for the Langmuir and Freundlich isotherms are summarized in Table 1. A plateau is observed at high equilibrium 2-ASP concentrations suggesting a Langmuir process may govern the sorption of dye to the sorbent, consistent with the purely electrostatic driven monolayer adsorption of positively charged 2-ASP over the negatively charged surface of HA-MNPs. Other studies related to dye removal also reported Langmuir as the best model for the equilibrium sorption (Chen et al., 2015; Guru and Dash, 2012; Li et al., 2019; Peng et al., 2012). The maximum adsorption capacity (qm) value obtained from the Langmuir model was 7.45 mg/g. A summary of the adsorption capacities of different dyes (malachite green, MG, methylene blue, MB and DO26) with different adsorbents is provided Table S5. The values in Table S5 indicates HA-MNPs have high potential for removing cationic pyridinium based styryl dyes from wastewater. where C₀ represents the initial dye concentration (mg L⁻¹) and K is Langmuir constant (L mg⁻¹). Dimensionless value of the R_L indicates the relative adsorption favorability of a system. For $0 < R_L < 1$ indicates favorable adsorption of dye molecules on HA-MNPs. Moreover, smaller values of R_L show the greater affinity between the adsorbent and the adsorbate (Gautam and Tiwari, 2020; Yan et al., 2013). The calculated R_L values are 0.035, 0.089 under our experimental conditions at an initial 2-ASP concentration of 25 mg/L, as listed in Table 1. These values are between 0 and 1, indicating favorable adsorption for 2-ASP under all explored experimental conditions.

3.5. Effect of pH

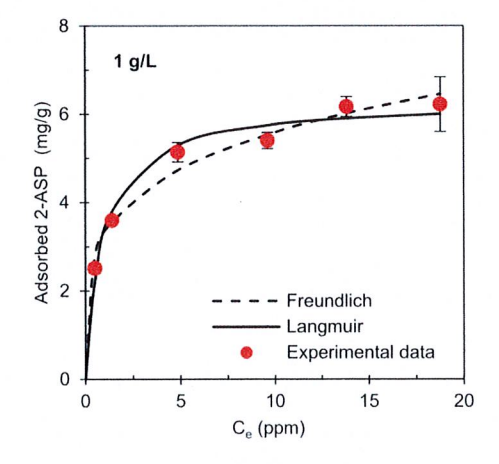
The adsorption of 2-ASP by HA-MNP was measured as a function of solution pH between 3 and 8 and results shown in Fig. S9. The overall

Table 1 Adsorption parameters and SSE based on nonlinear method.

$$R_{L} = \frac{1}{1 + KC_{0}} \tag{8}$$

HA-MNP (g/L)	Langmuir				Freundlich		
	K	q _m	SSE	R_L	k	n	SSE
1	1.09 ±	6.3 ±	0.409	0.035	3.29 ±	0.23 ±	0.341
	0.19	0.2			0.17	0.02	
2	$0.41 \pm$	$7.45 \pm$	0.207	0.089	$3.4 \pm$	$0.21 \pm$	0.388
	0.05	0.16			0.2	0.02	

Separation factor, R_L, for Langmuir isotherm, were calculated by Equation (8).



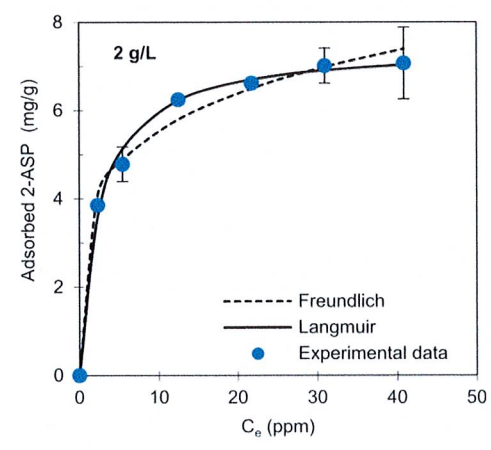


Fig. 2. Adsorption isotherm of 2-ASP on HA-MNPs. Initial dye concentration = 3–55 mg/L (ppm), pH = 7.1, HA-MNP dose = 1.0 g/L (left), 2 g/L (right), temperature = 298 K, contact time = 2 h.

removal increases from 40 % at pH = 3-66 % at pH = 7.5. In general, the sorption of dyes on the surface of the sorbent is significantly influenced by the pH, because changing in pH can affect speciation and the surface charge of the sorbent. The observed adsorption increase with increasing pH can be assigned to an enhanced electrostatic attraction between the positively charged 2-ASP and the increase in the negative charge on the HA-MNPs surface as a function of solution pH. At higher pH, modestly acidic groups (carboxylic, phenolic and hydroxyl groups) on the surface of the humic acid will be ionized increasing the overall negative charge on the HA-MNPs surface yielding a greater number of negative surface charges to participate in electrostatic attraction to the cationic dye. Whereas, under acidic conditions, when the solution pH is below pH_{PZC}, the surface charge of the HA-MNP becomes positive and thus can inhibit adsorption of positively charged absorbates. As a result, the sorption decreases. The increase in adsorption of a function of solution pH is not linear and may be related to individual pKa values of different functional groups present at the surface. This result agrees with various cationic dyes sorption to different sorbents such as humic acid coated magnetic nanoparticle (Gautam and Tiwari, 2020), biodegradable magnetic composite microsphere (Yan et al., 2013), magnetic biosorbent from peach gum polysaccharide (Li et al., 2018) and superparamagnetic Fe₃O₄ nanoparticles coated with green tea polyphenols (Singh et al., 2017).

3.6. Effect of sorbent dosage

The effect of sorbent dose on dye removal was studied at two different initial dye concentrations of 5 and 25 ppm, which demonstrated that the percent removal increases with sorbent dose, as the qe decreases (Fig. 3 a). This is rationalized as a competition of sorbents for sorption of the dye (Esmaeilian et al., 2015). With the total amount of dye at the desired concentration being constant, increasing the sorbent dose decreases the sorbate share per unit mass of the sorbent. In the other words, the number of active sites remaining unsaturated during the adsorption process is greater for higher sorbent doses. Fig. 3 b shows the rate of decrease is much faster in the 5 ppm concentration than the 25 ppm concentration as there is less dye and the competition is greater. This finding is consistent with reported literature (Kaouah et al., 2013; Rahimi et al., 2018).

3.7. Effect of temperature

To determine specific thermodynamic parameters associated with the adsorption process, the adsorption was measured with initial concentration of 5 ppm of 2-ASP (1 g/L of HA-MNPs) at different temperatures (22, 25, 30, 40, 45 and 55 $^{\circ}$ C) shown in Fig. S10. The adsorption only slightly increases with temperature. The modest increase in

adsorption is rationalized as an increase in molecular motions with the HA coating increasing the effective average pore size and increased flexibility of the adsorption sites on the surface with increasing temperature. The minimal effect of temperature observed is consistent with strictly electrostatic driven adsorption process since charge on the surface and dye does not appreciably change as a function of the temperatures studied.

3.8. Thermodynamic study

The thermodynamic parameters were determined using the Van't Hoff equation.

$$ln\left(\frac{q_e}{c_r}\right) = \frac{\Delta S}{R} - \frac{\Delta H}{RT} \tag{23}$$

where ΔH (kJ mol⁻¹), ΔS (J mol⁻¹K⁻¹) are the changes of enthalpy and entropy, respectively which can be calculated using the slope and intercept of plotting ln (q_e/C_e) versus 1/T (Fig. S11). Where q_e is the amount of 2-ASP dye adsorbed at equilibrium (mg/g), C_e is the equilibrium concentration (mg/L) of dye in solution, R is the ideal gas constant (8.314 J/K mol) and T is the temperature (K). The Gibbs free energy (ΔG) thus can be calculated as follows.

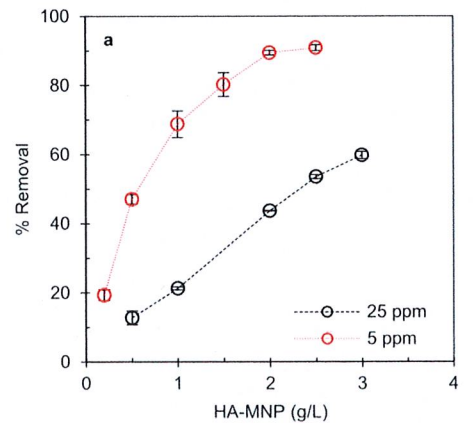
$$\Delta G = \Delta H - T \Delta S \tag{24}$$

The determined values of these thermodynamic parameters for our systems are $\Delta H = 7.7 \pm 0.2$ kJ/mol, $\Delta S = 31.6 \pm 0.8$ J/mol $^{\circ}$ K, and ΔG in J/mol $^{\circ}$ K increased with increasing temperature from -9.3 at 295 K to -10.4 at 328 K (Table S6).

The negative value of ΔG shows that sorption is spontaneous and thermodynamically favorable at all temperatures in this study. This finding is consistent with reported literature (Gautam and Tiwari, 2020). Therefore, no energy input is needed from outside of the system. The modest declining ΔG values with increasing temperature illustrate the adsorption becomes slightly more favorable at higher temperatures. The positive value of ΔS indicates that randomness of the system increases. Other studies showed the same pattern (Gautam and Tiwari, 2020; Somsesta et al., 2020).

4. Deducing a relationship for predicting removal efficiency by dimensional analysis

Isothermal studies for modeling adsorption generally employ constant sorbent dose. However, sorbent dose may affect the isotherm response. The equilibrium adsorbed dye is plotted versus equilibrium concentration confirming the effect of sorbent dose on isotherm shape illustrated in Fig. 4a. Moreover, removal is a function of initial concentration and sorbent dose, as depicted in Fig. 4b, without a specific



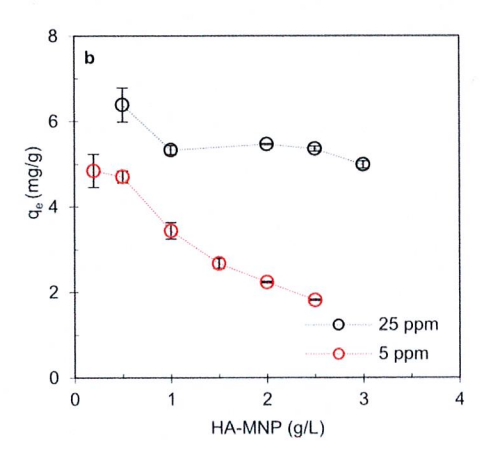


Fig. 3. The effect of sorbent dosage on (a) the removal of 2-ASP, (b) adsorbed dye.

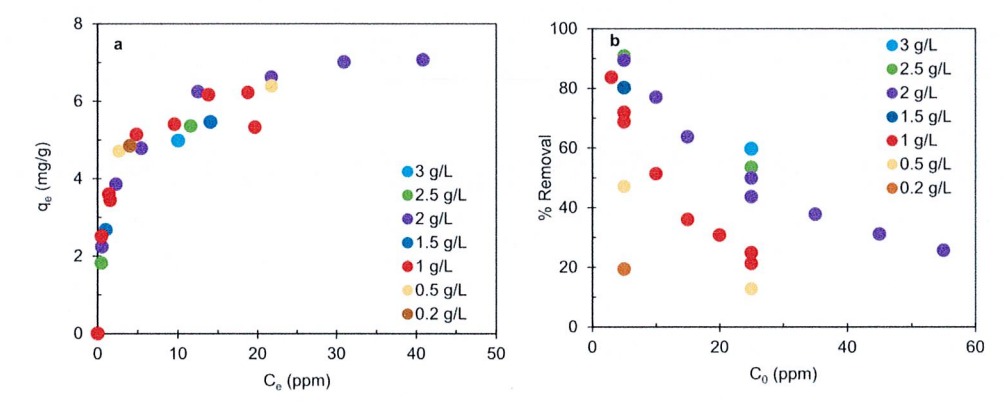


Fig. 4. The effect of sorbent dose on (a) isotherm: adsorbed dye, (b) removal of dye.

relationship between removal and initial concentration.

In this study, a generalized empirical model that considers C_0 and sorbent dose for isothermal study and removal efficiency prediction is deduced, using dimensional analysis employing Buckingham's π theorem (Chang and Wang, 2002; Rastogi et al., 2008).

Based on Buckingham's π theorem, a physical phenomenon which is a function of n variables, can be stated as a function of n-k dimensionless groupings in which k is the number of independent physical units (length, mass, and time). Based on different variables affecting the sorption process, one can consider following functional relationship for sorption:

$$f(C_0, C_e, W, V) = 0 (9)$$

where C_0 is initial concentration of dye (mg/L), C_e is the supernatant concentration at the equilibrium state of the system (mg/L), W is mass of humic acid coated magnetic nanoparticle (g) and V is the volume of the water (L).

Because in our study only length (L) and mass (M) units can be taken as fundamental units of measurement, the dimensions of the parameters will be as follow:

$$C_e = M/L^3$$
 $C_0 = M/L^3$ $V = L^3$ $W = M$ (10)

Considering C_0 and W as independent parameters, the following dimensionless groups were obtained:

$$\Pi_1 = \frac{C_e}{C_0} \tag{11}$$

$$\Pi_2 = \frac{C_0}{\text{Corbent dose}} \tag{12}$$

$$\Pi_1 = f(\Pi_2) \tag{13}$$

$$1 - \Pi_1 = 1 - f(\Pi_2) \tag{14}$$

Considering definition of \prod_1 in equation (11), one can conclude

$$\frac{C_0 - C_\epsilon}{C_0} = f_1(\Pi_2) \tag{15}$$

The right term of equation (15) is the definition of removal and by replacing \prod_2 using equation (12):

Removal (%) =
$$f\left(\frac{C_0}{Sorbent\ dose}\right)$$
 (16)

The removal percent versus C_0 /sorbent dose for all experimental data in this study is shown in Fig. 5.

In contrast to Fig. 4b, the data in Fig. 5 follow a unique equation (Equation (17)) that can predict removal efficiency as a function of initial concentration and sorbent dose with R² of 0.98.

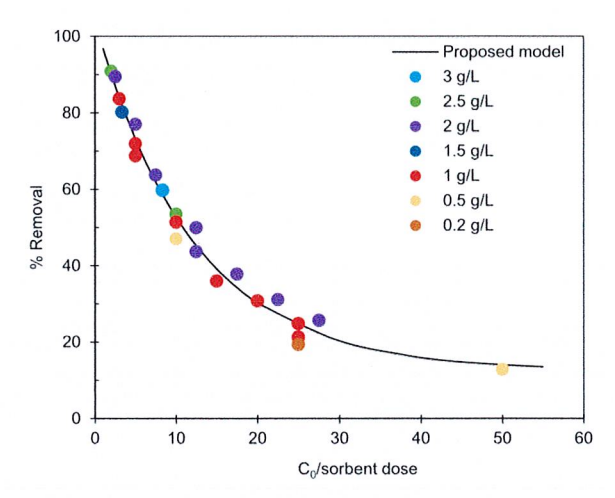


Fig. 5. Developing new equation for predicting removal.

$$Removal (\%) = 12.495 + 91.503 * e^{-0.082 \left(\frac{C_0}{Sorbent door}\right)}$$

$$(17)$$

If in Equation (9) C_e and W, are considered independent parameters, the following dimensionless groups are obtained:

$$\Pi_3 = \frac{C_0}{C_e} \tag{18}$$

$$\Pi_4 = \frac{C_e}{\text{Sorbent dose}} \tag{19}$$

Therefore,

$$\Pi_3 = f(\Pi_4) \tag{20}$$

By rearranging equation (20) and inserting \prod_3 and \prod_4 from Equations (18) and (19):

$$\frac{1}{\Pi_3} = f_1(\Pi_4) \rightarrow \frac{C_e}{C_0} = f\left(\frac{C_e}{Sorbent\ dose}\right)$$
 (21)

In Fig. 6, C_e/C_0 of the experimental data is plotted versus C_e /sorbent dose. In contrast to Fig. 4 a, the experimental data in Fig. 6 follow a unique equation with good correlation.

Therefore, for estimating equilibrium concentration based on sorbent dose an equation is developed (Equation (22)).

$$\frac{C_c}{C_0} = \frac{0.2390(C_c/Sorbent\ dosage)}{1 + 0.2672(C_c/Sorbent\ dosage)}$$
(22)

Dimensional analysis and experimental data showed that initial

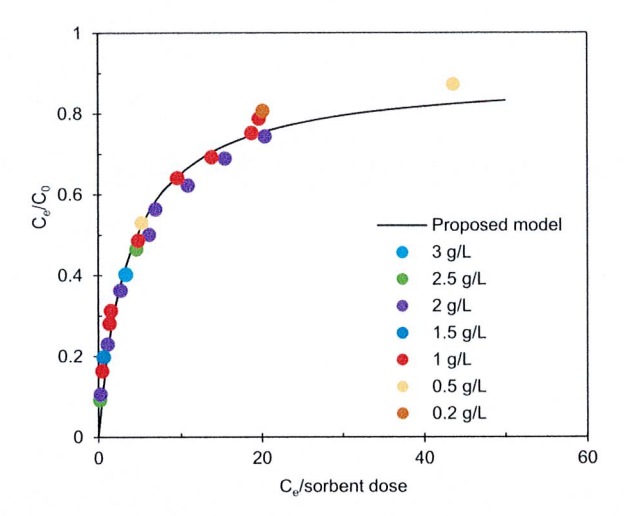


Fig. 6. Non dimensional relation between equilibrium and initial concentration and sorbent dose.

concentration/sorbent dose ratio should be considered while it is neglected in the literature. This approach is used to develop a mathematical model to predict the removal efficiency. This finding will help to reduce the number of sorption experiments and facilitate mathematical model development.

5. Regeneration and reusability of HA-MNPs

A method was developed to recover and regenerate HA-MNPs for cationic dye removal. HA-MNPs saturated with 2-ASP were subject to chemical treatment using a mixture of methanol and acetic acid at a 9:1 ratio for the desorption and regeneration. Although desorption of 2-ASP was fast using methanol, reuse of the recovered HA-MNPs showed low 2-ASP removal efficiency with a second cycle showing a ~50 % decrease in adsorption capacity (Fig. S12). This decrease can be attributed to protonation of functional groups effectively neutralizing the negative charges on the surface of HA-MNPs during the treatment with acetic acid. With the diminished number of negative charges present on the surface of the HA-MNPs there was a loss in potential for adsorption by electrostatic attraction between the sorbent and dye.

With this in mind, the regenerated adsorbent after treatment with methanol and acetic acid was titrated with 0.1 mol/L NaOH aqueous solution to bring solution pH 9.5 \pm 0.5. The resulting HA-MNPs were rinsed with deionized water until wash solution exhibited neutral pH. The regenerated alkaline treated HA-MNPs prepared from this procedure are referred to as recycled-HA-MNPs. The recycled-HA-MNPs were subject to five successive regeneration-adsorption cycles. The resultant adsorption performance of recycled-HA-MNPs in successive regeneration-adsorption cycles is compared with the original adsorption capacity was illustrated in Fig. S12. As shown in Fig. S12, the removal efficiency of HA-MNPs increased ~25 % compared with original HA-MNPs. The observed increase in adsorption capacity may be the result of hydrolysis processes initiated by the alkaline conditions employed in the regeneration process yielding an increase in the number carboxylates present in the HA surface via hydrolysis of esters and amides effectively increasing the overall negative charge at the surface of the HA-MNPs enhancing potential for adsorption of cations. The removal efficiency by the recycled-HA-MNPs remained constant even after the 5th regeneration cycle maintaining high adsorption capacity and stability for repeated adsorption of cationic dyestuffs. The methanol, acetic acid and 2-ASP could be recovered, reused and/or treated depending on economic assessment (Zhang et al., 2013).

The potential of alkaline treatment to enhance adsorption capacity has been observed in different sorbents. Ashrafi et al. showed that NaOH-modified rice husk (NaOH-RH) has a great potential for direct red 81 and methylene blue adsorption (Ashrafi et al., 2016). In another study, NaOH-activated carbon demonstrated a high capacity for removal of methylene blue, basic brown, and acid blue 74 from wastewater (Wu and Tseng, 2008).

Our results show the adsorption equilibrium time of recycled-HA-MNPs is reduced. This may be the result of reduced agglomeration and/or less cationic bridging of particles due to increased negative surface charge on the HA-MNPs. Therefore, increasing effective surface area leading to faster adsorption kinetics. The application of a co-solvent of acetic acid/methanol in combination with NaOH treatment for regeneration is excellent process for regenerating of HA-MNPs (Zhang et al., 2013). The schematic of batch adsorption-desorption experiments is illustrated in Fig. S13.

The recycled-HA-MNPs were characterized exhibiting the pH of zeropoint charge (pH_{PZC}) decreased to ~ 2.2 compared with the pH_{PZC} of native HA-MNPs (pH_{PZC} = 3.7). The low pH_{PZC} indicates that the recycled-HA-MNPs are negatively charged across the environmentally relevant acidity (pH 2-9), which inhibits the aggregation of HA-MNPs and enhances the sorption of positively charged species (Fig. S14). The ATR-FTIR spectra of original HA-MNPs and recycled-HA-MNPs are shown in Fig. S15. The peaks at $\sim 600 \text{ cm}^{-1}$ (Fe–O), 1565 cm⁻¹ (C=O stretching), and 1373 cm⁻¹ (-CH₂ group) in both coated and treated magnetic nanoparticles were observed, indicating no significant change in the structure and functional groups after treating with NaOH. Results of this study showed that treatment of the as-prepared HA-MNPs before the adsorption is an important modification of HA-MNPs. The regeneration of HA-MNPs without loss of adsorption capacity up to 5 regeneration cycles, implies the stability and excellent recyclability of the HA-MNPs. Therefore, this regeneration technique can be useful for increasing the HA-MNPs adsorption capacity.

6. Conclusions

Environmentally friendly humic acid coated magnetic nanoparticles effectively remove of carcinogenic cationic 2-ASP dye from wastewater. The adsorption kinetics and adsorption isotherms exhibit pseudo 2nd order is the suitable model and adsorption happened on the monolayer of the nanoparticles. Thermal experiments provided the evidence that adsorption of 2-ASP onto absorbent HA-MNP was favorable, endothermic and spontaneous. The results showed that both initial concentration and sorbent dose effects the sorption process. Dimensional analysis along with experimental data suggest that ratio of initial concentration and sorbent dose should be considered as a variable in prediction of removal efficiency. Unique equation that predicts removal efficiency as a function of initial concentration and sorbent dose ratio with R² of 0.98 were deduced by dimensional analysis. This new finding will help researchers in sorption studies to design their experiments more efficiently and to develop improved empirical models in removal prediction. The removal efficiency by regenerated HA-MNPs remained constant up to 5 regeneration cycles. The proposed novel method for regeneration of HA-MNPs showed that NaOH treatment prior to adsorption may be an efficient approach in modifying the HA-MNPs surface and enhancing the maximum adsorption capacity and removal efficiency. Removal efficiency of treated HA-MNPs with NaOH increase \sim 25 % compared with original HA-MNPs. Finally, this study provides a better understanding of the adsorption process of styryl dyes, which is valuable as such dyes are an important contaminant in the effluent of textile industries. Future studies are needed to evaluate adsorption to this nanoparticle of different types of dyes which are a great concern in water pollution in developing countries. These results shine a light on necessary parameters for designing the wastewater treatment system for decontamination of wastewater. Positive downstream environmental impacts combined with the economic efficiency of incorporating this into a filtration process make this application of nanotechnology feasible for future use.

Chemosphere 286 (2022) 131699 A. Esmaeilian and K.E. O'Shea

Credit author statement

Anahita Esmaeilian: Validation, Visualization, Formal analysis, Investigation, Writing - Original Draft, Creation of models Kevin E. O'Shea Conceptualization, Development or design of methodology; Resources, Writing - Review & Editing, Supervision, Project administration, Funding acquisition.

Declaration of competing interest

The authors declare that they have no known competing financial interests or personal relationships that could have appeared to influence the work reported in this paper.

Acknowledgements

This research was funded by the National Science Foundation under [Grants Number CHE-1710111 and 1905239]. This material is also based upon work supported by the National Science Foundation under [Grant Number HRD-1547798]. This NSF Grant was awarded to Florida International University as part of the Centers of Research Excellence in Science and Technology (CREST) Program. This is contribution number 1014 from the Southeast Environmental Research Center in the Institute of Environment at Florida International University.

Appendix A. Supplementary data

Supplementary data to this article can be found online at https://doi. org/10.1016/j.chemosphere.2021.131699.

References

- Al-Degs, Y.S., Sweileh, J.A., 2012. Simultaneous determination of five commercial cationic dyes in stream waters using diatomite solid-phase extractant and multivariate calibration. Arab. J. Chem. 5, 219-224. https://doi.org/10.1016/j. arabjc,2010.08.016.
- Allen, S.J., Koumanova, B., 2005. Decolourisation of water/wastewater using adsorption. J. Univ. Chem. Technol. Metall. 40, 175-192.
- Ashrafi, S.D., Kamani, H., Mahvi, A.H., 2016. The optimization study of direct red 81 and methylene blue adsorption on NaOH-modified rice husk. Desalin. Water Treat. 57, 738-746. https://doi.org/10.1080/19443994.2014.979329.
- Azizian, S., 2004. Kinetic models of sorption: a theoretical analysis. J. Colloid Interface Sci. 276, 47-52. https://doi.org/10.1016/j.jcis.2004.03.048.
- Bahrudin, N.N., Nawi, M.A., Sabar, S., 2019. Immobilized chitosan-montmorillonite composite adsorbent and its photocatalytic regeneration for the removal of methyl orange. React. Kinet. Mech. Catal. 126, 1135-1153. https://doi.org/10.1007/ s11144-019-01536-6
- Bayramoglu, G., Altintas, B., Arica, M.Y., 2009. Adsorption kinetics and thermodynamic parameters of cationic dyes from aqueous solutions by using a new strong cationexchange resin. Chem. Eng. J. 152, 339-346. https://doi.org/10.1016/j cej.2009.04.051
- Boparai, H.K., Joseph, M., O'Carroll, D.M., 2011. Kinetics and thermodynamics of cadmium ion removal by adsorption onto nano zerovalent iron particles. J. Hazard Mater. 186, 458-465. https://doi.org/10.1016/j.jhazmat.2010.11.029.
- Brahim, I.O., Belmedani, M., Hadoun, H., Belgacem, A., 2021. The photocatalytic degradation kinetics of food dye in aqueous solution under UV/ZnO system. React. Kinet. Mech. Catal. 2021, 1-21. https://doi.org/10.1007/S11144-021-02006-
- Chang, T.W., Wang, M.K., 2002. Assessment of sorbent/water ratio effect on adsorption using dimensional analysis and batch experiments. Chemosphere 48, 419-426 https://doi.org/10.1016/S0045-6535(02)00053-X.
- Chen, R.P., Zhang, Y.L., Wang, X.Y., Zhu, C.Y., Ma, A.J., Jiang, W.M., 2015. Removal of methylene blue from aqueous solution using humic-acid coated magnetic nanoparticles. Desalin. Water Treat. 55, 539-548. https://doi.org/10.1080/ 19443994.2014.916233.
- Deng, H., Yin, J., Ma, J., Zhou, J., Zhang, L., Gao, L., Jiao, T., 2021. Exploring the enhanced catalytic performance on nitro dyes via a novel template of flake-network Ni-Ti LDH/GO in-situ deposited with Ag3PO4 NPs. Appl. Surf. Sci. 543, 148821. https://doi.org/10.1016/j.apsusc.2020.148821
- Ding, W., Guo, S., Liu, H., Pang, X., Ding, Z., 2021. Synthesis of an amino-terminated waterborne polyurethane-based polymeric dye for high-performance dyeing of biomass-derived aldehyde-tanned chrome-free leather. Mater. Today Chem. 21, 100508. https://doi.org/10.1016/J.MTCHEM.2021.100508
- Esmaeilian, A., Mahdavi Mazdeh, A., Ghaforian, H., Liaghat, A.M., 2015. A novel nanopore biopolymer multi adsorbent for simultaneous removal of anionic and cationic mixtures. Desalin. Water Treat. 53, 2235-2248. https://doi.org/10.1080/ 19443994.2013.861772.

Freundlich, H.M.F., 1906. Ueber die adsorption in loesungen. J. Phys. Chem. 57,

- Gautam, R.K., Tiwari, I., 2020. Humic acid functionalized magnetic nanomaterials for remediation of dye wastewater under ultrasonication: application in real water samples, recycling and reuse of nanosorbents. Chemosphere 245, 125553. https:// doi.org/10.1016/j.chemosphere.2019.125553
- Ge, F., Ye, H., Li, M.-M., Zhao, B.-X., 2012. Efficient removal of cationic dyes from aqueous solution by polymer-modified magnetic nanoparticles. Chem. Eng. J. 198-199, 11-17. https://doi.org/10.1016/j.cej.2012.05.074.
- Guru, P.S., Dash, S., 2012. Eggshell particles (ESP) as potential adsorbent for styryl pyridinium dyes-A kinetic and thermodynamic study. J. Dispersion Sci. Technol. 33, 1012-1020. https://doi.org/10.1080/01932691.2011.590750.
- Ho, Y.-S., 2006. Second-order kinetic model for the sorption of cadmium onto tree fern: a comparison of linear and non-linear methods. Water Res. 40, 119-125. https://doi. org/10.1016/j.watres.2005.10.040.
- Ho, Y.S., McKay, G., 1999. Pseudo-second order model for sorption processes. Process Biochem. 34, 451–465. https://doi.org/10.1016/S0032-9592(98)00112-5. Ho, Y.S., McKay, G., 1998. A comparison of chemisorption kinetic models applied to
- pollutant removal on various sorbents. Trans IChemE 76, 332-340.
- Huang, X., Wang, R., Jiao, T., Zou, G., Zhan, F., Yin, J., Zhang, L., Zhou, J., Peng, Q., 2019. Facile preparation of hierarchical AgNP-loaded MXene/Fe3O4/polymer nanocomposites by electrospinning with enhanced catalytic performance for wastewater treatment. ACS Omega 4, 1897-1906. https://doi.org/10.1021/ ACSOMEGA.8B03615.
- Kaouah, F., Boumaza, S., Berrama, T., Trari, M., Bendjama, Z., 2013. Preparation and characterization of activated carbon from wild olive cores (oleaster) by H3PO4 for the removal of Basic Red 46. J. Clean. Prod. 54, 296-306. https://doi.org/10.1016/j iclepro, 2013, 04, 038
- Kausar, A., Shahzad, R., Asim, S., BiBi, S., Iqbal, J., Muhammad, N., Sillanpaa, M., Din, I. U., 2021. Experimental and theoretical studies of Rhodamine B direct dye sorption onto clay-cellulose composite. J. Mol. Liq. 328, 115165. https://doi.org/10.1016/J. MOLLIO, 2020, 115165.
- Kavitha, D., Namasivayam, C., 2007. Experimental and kinetic studies on methylene blue adsorption by coir pith carbon. Bioresour. Technol. 98, 14-21. https://doi.org/
- Konicki, W., Helminiak, A., Arabczyk, W., Mijowska, E., 2017. Removal of anionic dyes using magnetic Fe@graphite core-shell nanocomposite as an adsorbent from aqueous solutions. J. Colloid Interface Sci. 497, 155-164. https://doi.org/10.1016/j.
- Langmuir, I., 1918. The adsorption of gases on plane surfaces of mica. J. Am. Chem. Soc. 40, 1361-1403. https://doi.org/10.1021/ja01269a066.
- Li, C., Wang, X., Meng, D., Zhou, L., 2018. Facile synthesis of low-cost magnetic biosorbent from peach gum polysaccharide for selective and efficient removal of cationic dyes. Int. J. Biol. Macromol. 107, 1871-1878. https://doi.org/10.1016/j. iibiomac, 2017, 10, 058.
- Li, Q., Zhan, Z., Jin, S., Tan, B., 2017. Wettable magnetic hypercrosslinked microporous nanoparticle as an efficient adsorbent for water treatment. Chem. Eng. J. 326, 109-116. https://doi.org/10.1016/j.cej.2017.05.049.
- Li, Z., Sun, Y., Xing, J., Meng, A., 2019. Fast removal of methylene blue by Fe 3 O 4 magnetic nanoparticles and their cycling property. J. Nanosci. Nanotechnol. 19, 2116-2123. https://doi.org/10.1166/jnn.2019.15809.
- Liu, J., Zhao, Z., Jiang, G., 2008. Coating Fe₃ O₄ magnetic nanoparticles with humic acid for high efficient removal of heavy metals in water, 42, 6949–6954.
- Mahdayi, A., Kashefipour, S.M., Omid, M.H., 2013. Effect of sorption process on cadmium transport. Proc. Inst. Civ. Eng. - Water Manag. 166, 152-162. https://doi. org/10.1680/wama.11.00040.
- Malik, P.K., 2004. Dye removal from wastewater using activated carbon developed from sawdust: adsorption equilibrium and kinetics. J. Hazard Mater. 113, 81-88. https:// doi.org/10.1016/j.jhazmat.2004.05.022.
- Nasrabadi, M., Omid, M.H., Mahdavi, A., 2017. Cadmium adsorption characteristics for karaj riverbed sands. J. Mater. Environ. Sci. 8, 1729-1736
- Nunamaker, E.A., Otto, K.J., Artwohl, J.E., Fortman, J.D., 2013. Leaching of heavy metals from water bottle components into the drinking water of rodents. JAALAS 52 (1), 22-27. PMCID: PMC3548197.
- Oseroff, A.R., Ohuoha, D., Ara, G., McAuliffe, D., Foley, J., Cincotta, L., 1986. Intramitochondrial dyes allow selective in vitro photolysis of carcinoma cells. Proc. Natl. Acad. Sci. Unit. States Am. 83, 9729-9733. https://doi.org/10.1073/ onas,83,24,9729.
- Parida, S.K., Dash, S., Patel, S., Mishra, B.K., 2006. Adsorption of organic molecules on silica surface. Adv. Colloid Interface Sci. 121, 77-110. https://doi.org/10.1016/j.
- Peng, L., Qin, P., Lei, M., Zeng, Q., Song, H., Yang, J., Shao, J., Liao, B., Gu, J., 2012. Modifying Fe3O4 nanoparticles with humic acid for removal of Rhodamine B in water. J. Hazard Mater. 209-210, 193-198. https://doi.org/10.1016/j. jhazmat.2012.01.011.
- Puvaneswari, N., Muthukrishnan, J., Gunasekaran, P., 2006. Toxicity assessment and microbial degradation of azo dyes. Indian J. Exp. Biol. 44, 618-626.
- Qian, C., Yin, J., Zhao, J., Li, X., Wang, S., Bai, Z., Jiao, T., 2021. Facile preparation and highly efficient photodegradation performances of self-assembled Artemia eggshell-ZnO nanocomposites for wastewater treatment. Colloids Surfaces A Physicochem. Eng. Asp. 610, 125752. https://doi.org/10.1016/j.colsurfa.2020.125752.
- Rahimi, K., Mirzaei, R., Akbari, A., Mirghaffari, N., 2018. Preparation of nanoparticlemodified polymeric adsorbent using wastage fuzzes of mechanized carpet and its application in dye removal from aqueous solution. J. Clean. Prod. 178, 373-383. https://doi.org/10.1016/j.jclepro.2017.12.213.

Rashid, M., Price, N.T., Angel, M., Pinilla, G., Shea, K.E.O., 2017. Effective removal of phosphate from aqueous solution using humic acid coated magnetite nanoparticles 123, 353–360. https://doi.org/10.1016/j.watres.2017.06.085.

- Rashid, M., Sterbinsky, G.E., Pinilla, M.Á.G., Cai, Y., O'Shea, K.E., 2018. Kinetic and mechanistic evaluation of inorganic arsenic species adsorption onto humic acid grafted magnetite nanoparticles. J. Phys. Chem. C 122, 13540–13547. https://doi. org/10.1021/acs.jpcc.7b12438.
- Rastogi, K., Sahu, J.N., Meikap, B.C., Biswas, M.N., 2008. Removal of methylene blue from wastewater using fly ash as an adsorbent by hydrocyclone. J. Hazard Mater. 158, 531–540. https://doi.org/10.1016/j.jhazmat.2008.01.105.
- Sakti, S.C.W., Laily, R.N., Aliyah, S., Indrasari, N., Fahmi, M.Z., Lee, H.V., Akemoto, Y., Tanaka, S., 2020. Re-collectable and recyclable epichlorohydrin-crosslinked humic acid with spinel cobalt ferrite core for simple magnetic removal of cationic triarylmethane dyes in polluted water. J. Environ. Chem. Eng. 8, 104004. https://doi.org/10.1016/j.jece.2020.104004.
- Shahriari, T., Mazdeh, A.M., Omid, M.H., Nasrabadi, M., 2018. Cadmium adsorption by natural zeolite in a circular flume. Int. J. Environ. Technol. Manag. 21, 174. https://doi.org/10.1504/JJETM.2018.10019130.
- Singh, K.K., Senapati, K.K., Sarma, K.C., 2017. Synthesis of superparamagnetic Fe3O4 nanoparticles coated with green tea polyphenols and their use for removal of dye pollutant from aqueous solution. J. Environ. Chem. Eng. 5, 2214–2221. https://doi.org/10.1016/j.jece.2017.04.022.
- Sohni, S., Hashim, R., Nidaullah, H., Lamaming, J., Sulaiman, O., 2019. Chitosan/nanolignin based composite as a new sorbent for enhanced removal of dye pollution from aqueous solutions. Int. J. Biol. Macromol. 132, 1304–1317. https://doi.org/10.1016/j.ijbiomac.2019.03.151.
- Somsesta, N., Sricharoenchaikul, V., Aht-Ong, D., 2020. Adsorption removal of methylene blue onto activated carbon/cellulose biocomposite films: equilibrium and kinetic studies. Mater. Chem. Phys. 240, 122221. https://doi.org/10.1016/j. matchemphys.2019.122221.

- Vermeer, A.W.P., Van Riemsdijk, W.H., Koopal, L.K., 1998. Adsorption of humic acid to mineral particles. 1. Specific and electrostatic interactions. Langmuir 14, 2810–2815. https://doi.org/10.1021/la970624r.
- Wu, F.-C., Tseng, R.-L., 2008. High adsorption capacity NaOH-activated carbon for dye removal from aqueous solution. J. Hazard Mater. 152, 1256–1267. https://doi.org/ 10.1016/j.jhazmat.2007.07.109.
- Yan, H., Li, H., Yang, H., Li, A., Cheng, R., 2013. Removal of various cationic dyes from aqueous solutions using a kind of fully biodegradable magnetic composite microsphere. Chem. Eng. J. 223, 402–411. https://doi.org/10.1016/j. cej.2013.02.113.
- Zhang, X., Zhang, P., Wu, Z., Zhang, L., Zeng, G., Zhou, C., 2013. Adsorption of methylene blue onto humic acid-coated Fe3O4 nanoparticles. Colloids Surfaces A Physicochem. Eng. Asp. 435, 85–90. https://doi.org/10.1016/j. colsurfa.2012.12.056.
- Zhang, Y., Yin, M., Sun, X., Zhao, J., 2020. Implication for adsorption and degradation of dyes by humic acid: light driven of environmentally persistent free radicals to activate reactive oxygen species. Bioresour. Technol. 307, 123183. https://doi.org/ 10.1016/j.biortech.2020.123183.
- Zhao, H., Wang, R., Deng, H., Zhang, Lijun, Gao, L., Zhang, Lexin, Jiao, T., 2021. Facile preparation of self-assembled chitosan-based POSS-CNTs-CS composite as highly efficient dye absorbent for wastewater treatment. ACS Omega 6, 294–300. https://doi.org/10.1021/acsomega.0c04565.
- Zhou, Yanbo, Lu, J., Zhou, Yi, Liu, Y., 2019. Recent advances for dyes removal using novel adsorbents: a review. Environ. Pollut. 252, 352–365. https://doi.org/10.1016/ i.envnol.2019.05.072.
- Zhu, M., Sun, Z., Fujitsuka, M., Majima, T., 2018. Z-scheme photocatalytic water splitting on a 2D heterostructure of black phosphorus/bismuth vanadate using visible light. Angew. Chem. Int. Ed. 57, 2160–2164. https://doi.org/10.1002/ANIE.201711357.